Applied Catalysis B: Environmental 83 (2008) 256–264

Contents lists available at ScienceDirect

Applied Catalysis B: Environmental

journal homepage: www.elsevier.com/locate/apcatb

Catalytic ozonation for the degradation of nitrobenzene in aqueous solution by ceramic honeycomb-supported manganese

Lei Zhao [a,*], Jun Ma [a,**], Zhi-zhong Sun [b], Xue-dong Zhai [a]

[a] School of Municipal and Environmental Engineering, Harbin Institute of Technology, 202 Haihe Road, Harbin 150090, People's Republic of China
[b] School of Chemistry and Materials Science, Heilongjiang University, Harbin 150080, People's Republic of China

ARTICLE INFO

Article history:
Received 27 November 2007
Received in revised form 13 February 2008
Accepted 15 February 2008
Available online 20 February 2008

Keywords:
Catalytic ozonation
Nitrobenzene
Ceramic honeycomb
Mn
Hydroxyl radical (•OH)

ABSTRACT

Catalytic ozonation of nitrobenzene in aqueous solution has been carried out in a semi-continuous laboratory reactor where ceramic honeycomb and Mn–ceramic honeycomb have been used as the catalysts. The presences of the two catalysts significantly improve the degradation efficiency of nitrobenzene, the utilization efficiency of ozone and the production of oxidative intermediate species compared to the results from non-catalytic ozonation, and the improvement of them is even more pronounced in the presence of Mn–ceramic honeycomb. Adsorptions of nitrobenzene on the two catalytic surfaces have no remarkable influence on the degradation efficiency. Addition of *tert*-butanol causes the obvious decrease of degradation efficiency, suggesting that degradation of nitrobenzene follows the mechanism of hydroxyl radical (•OH) oxidation. Some of the main operating variables like amount of catalyst and reaction temperature exert a positive influence on the degradation efficiency of nitrobenzene. Initial pH also presents a positive effect in the ozonation alone system while the optimum working initial pH is found to be around 8.83 and 10.67 to the processes of ozonation/ceramic honeycomb and ozonation/Mn–ceramic honeycomb, respectively. The surface characteristics measurement of the two catalysts indicates that the loading of Mn increases the specific surface area, the pH at the point of zero charge (pH_{PZC}) and the density of surface hydroxyl groups, and results in the appearance of new crystalline phase of MnO_2. The results of mechanism research confirm that the loading of Mn promotes the initiation of •OH.

1. Introduction

Nitrobenzene is a major environmental pollutant due to its carcinogenesis and mutagenesis [1,2]. The commercial uses of nitrobenzene are reduction to aniline, solvent, synthetic products of benzene [3], metal polishes, shoe-black, perfume, dye intermediates [4,5], plastics, explosives, pharmaceuticals [6], pesticides [7] and a combustible propellant [1]. The production of nitrobenzene in the USA was close to 0.75 billion kg for the year 1995 [1]. Therefore, the remediation of nitrobenzene in aqueous solution is of environmental concern because of its toxicity and the quantity of its production. However, nitrobenzene resists to oxidation by conventional chemical oxidation due to the strong electron-withdrawing property of the nitro-group. Mineralization of nitrobenzene by microorganisms is prevented owing to the effects of toxic and mutagenic on biological systems, which derive from nitrobenzene and its transformation metabolites, such as nitrosobenzene, hydroxylaminobenzene and aniline [2,4,8–16]. In order to afford the inexpensive and effective processes for the water treatment, various chemical reduction treatment and advanced oxidation processes (AOPs) have been studied for the degradation of nitrobenzene in aqueous solution, such as Fe^0 reduction [1,2], photocatalysis [17,18], photoassisted Fenton oxidation [19], supercritical oxidation [20] and so on.

AOPs are characterized by the generation of hydroxyl radical (•OH), species of high oxidizing power, that reacts on the matter present in water in an unselective way [21]. In recent years, heterogeneous catalytic ozonation, as a promising AOP, has received much attention in water treatment due to its high oxidation potential. Several researches have been reported on the degradation of nitrobenzene in aqueous solution by the heterogeneous catalytic ozonation processes. The experimental results indicate that removal efficiency of nitrobenzene is significantly promoted in the presence of heterogeneous catalysts compared

* Corresponding author. Tel.: +86 451 82291644 or 86 451 86283010; fax: +86 451 82368074.
** Corresponding author. Tel.: +86 451 86282292 or 86 451 86283010; fax: +86 451 82368074.
E-mail addresses: zhaolei999999@126.com (L. Zhao), majun@hit.edu.cn (J. Ma).

0926-3373/$ – see front matter © 2008 Elsevier B.V. All rights reserved.
doi:10.1016/j.apcatb.2008.02.009

with that of ozone alone, including nano-TiO_2 [22], Mn-loaded granular activated carbon (MnO_x/GAC) [23,24], ceramic honeycomb [25,26] and synthetic goethite [27]. Moreover, except for MnO_x/GAC catalytic ozonation, it is found that the degradation of nitrobenzene follows the •OH oxidation mechanism in the other systems mentioned above.

In order to increase the catalytic activity of ceramic honeycomb [25,26] and develop the convenient operation of manganese catalyst [23,28–30] used in the previous study, ceramic honeycomb was modified by loading Mn in the experiments, and the degradation efficiency of organic micropollutant was investigated by ceramic honeycomb-supported Mn catalytic ozonation. Nitrobenzene slowly reacts with molecular ozone ($0.09 \pm 0.02\ M^{-1}\ s^{-1}$), reacts quickly with •OH ($2.2 \times 10^8\ M^{-1}\ s^{-1}$) and it does not adsorb on the ceramic honeycomb catalyst surface. Therefore, nitrobenzene, listed as a priority pollutant, is chosen as a model pollutant due to its toxicity of the central nervous system and its refractory nature to conventional chemical oxidation, and the special indication of •OH. Furthermore, the objective of the present investigation was to compare the degradation efficiency of nitrobenzene in the different processes (ozonation alone, catalytic ozonation and adsorption of catalysts), and to elucidate several control options for the degradation efficiency of nitrobenzene (addition of •OH scavenger, amount of catalyst, reaction temperature, initial pH) and to confirm preliminarily the reaction mechanism.

2. Materials and methods

2.1. Materials and reagents

Monoliths of ceramic honeycomb (Shanghai Pengyinaihuo Material Factory, China) were used as the catalyst and the framework of catalyst. These blocks have the following characteristics: the shape of a cylinder with a diameter of 50 mm and a length of 50 mm, wall thickness 0.4 mm, the cell density 400 square cells per square inch and the weight of a single block of ceramic honeycomb was 34.6–35.4 g. All the monolithic blocks were cleaned before the catalytic ozonation process and the modified procedure by immersing them into a vessel with redistilled water, which was placed into an ultrasonic bath during 10 min. Afterwards, they were dried in a stove at 393 K overnight, and then stored in a dry vacuum oven for use.

The model water was prepared by spiking 50 $\mu g\ L^{-1}$ nitrobenzene (Beijing Chemical Factory, China, purified by distillation pretreatment, 99.80%) in Milli-Q water (Millipore Q Biocel system). *tert*-Butanol was purchased from Beijing Chemical Co. Ltd., and used without further purification. Perchloric acid (Tianjin Dongli Chemical Factory of Tianjin University, China) and sodium hydroxide (Harbin Xinchun Chemical Factory, China) were added in aqueous solution to control the pH. Manganese nitrate (50% w/w solution, Beijing Chemical Factory, China), and all other chemicals used in the experiments were analytical grade reagents. A diluted sodium thiosulphate solution was used in the experiments for quenching the reaction. All the glassware except for volumetric flasks was muffled overnight at 673 K. The volumetric flasks were washed by soaking them in chromic acid and then rinsing with distilled water.

2.2. Catalyst preparation

The modified procedure was carried out via wet impregnation of the monolithic blocks with appropriate concentrations of metal ions in an aqueous solution of manganese nitrate salt over a period of 4 h. The optimization experiments were carried out at various concentrations of impregnation solution (0.5–50.0%), temperature (423–1023 K) and time (0.5–8.0 h) of calcination to attain the optimizing conditions, which were listed as follows. The concentration of $Mn(NO_3)_2$ was 6.0%, the unique amount determined through the optimizing experiments. Impregnated blocks were dried at room temperature for 12 h in air, then at 393 K for 12 h, and calcined at 723 K for 4 h. The procedure was repeated until the wash-coat loading reached the target loading percentage of the total monolith weight.

2.3. Ozonation procedure

The experiments were carried out in a cylindrical ozonation reactor (the inside diameter of 50 mm and the volume of 3 L) made of stainless steel, which was shielded to control reaction temperature constantly at 293 K using a thermostatic bath (DC-2015, Ningbo Tianheng Instruments Factory, China) and flow through a surrounding water jacket. Ozone was produced from pure oxygen (Harbin Gas Co. Ltd., 99.999%, China) through XFZ-5 ozone generator (Qinghua Tongli, China) at a power setting of 40 W, and was subsequently fed into the ozonation reactor to contact thoroughly with water samples through a porous titanium sand plate at the bottom of the reactor. The concentration of total applied ozone in this experiment was controlled at 1.00 $mg\ L^{-1}$. Before the experimental operation, the reactor was pre-ozonated for 4 min to satisfy any ozone demand in the column and then was washed several times with twice-distilled water to exclude possible side effects. In the ozonation tests, the model water (3 L), preparing by spiking 50 $\mu g\ L^{-1}$ nitrobenzene in Milli-Q water, was pumped into the ozonation reactor by means of an MP-20R magnetic pump (Shanghai Xishan Pump Co. Ltd., China) and then circulated at a rate of approximately 2 $L\ min^{-1}$. The ceramic honeycomb catalysts were fed into the reactor by taking off its base. The ozonation time was controlled at 15 min for every batch experiment. Water samples were taken from the reactor at various reaction times to analyze the residual concentration of nitrobenzene. The oxidation reaction was quenched by the addition of a small amount of sodium thiosulphate solution.

2.4. Analytical method

Typically a 50-mL sample containing nitrobenzene was extracted using a total volume of 1-mL benzene (Tianjin Kemiou Research and Development Centre of Chemicals, China, HPLC Grade). Nitrobenzene was analyzed by injecting 1 μL of the extracted headspace sample into GC-14C gas chromatography spectrometer (Shimadzu, Japan), using the high purity nitrogen (99.99%) as the mobile phase at a rate of 34 $mL\ min^{-1}$. The conditions of GC-14C gas chromatography were as follows: column temperature: 433 K; injector and detector temperature: 483 K. The pH of aqueous solution was measured by PB-10 pH meter (Sartorious, Germany).

The concentration of ozone in the gas was measured by iodometric titration method [31]. The concentration of residual ozone in aqueous solution was measured by spectrophotometer using the indigo method [32]. The concentration of H_2O_2 formed in the oxidation system was determined by the photometric method [33].

X-ray power diffraction (XRD, Input Gokv Zokw Co. Ltd., Japan, Model A-41L-Cu) was used to analyze the crystal phase of the catalysts in monochromatized Cu Kα radiation using curved graphite monochromator on diffracted beam with operating voltage of 45 kV and current of 50 mA.

The specific surface area of the catalyst samples were measured according to the Brunauer–Emmet–Teller (BET) method with the krypton adsorption at liquid nitrogen temperature on a Micromeritics ASAP 2020. To measure the BET specific surface area of the

catalyst monoliths, a particular home-made test tube was needed to host the sample.

The density of surface hydroxyl groups was measured according to a saturated deprotonation method described by Laiti and Tamara [34,35]. The pH at the point of zero charge (pH_{PZC}) was measured with a mass titration method [36,37].

Electron paramagnetic resonance (EPR) experiment was conducted for the determination of •OH generated in the ozonation process [22]. A nitron spin-trapping reagent of 5,5-dimethyl-1-pyrolin-*N*-oxide (DMPO), which was purchased from Fluka, was used in the process. In succession, the EPR spectrum was measured at room temperature with an EPR spectrometer (Bruker EMX-8/2.7 ESR 8 spectrometer with ER 4102ST cavity) under the following experimental conditions: X-Field Sweep; Center Field 3480.00 G; Sweep Width 100.00 G; Static Field 3480.00 G; Frequency 9.751000 GHz; Power 4.00 mW. The sample was scanned and accumulated 10 times for 20.972 × 10 s.

3. Results and discussion

3.1. Degradation efficiency of nitrobenzene in the different processes

The experiments were performed in the different processes to investigate the degradation efficiency of nitrobenzene, including ozonation alone, ozonation/ceramic honeycomb, ozonation/Mn–ceramic honeycomb, adsorption of ceramic honeycomb and adsorption of Mn–ceramic honeycomb, under the condition of the applied specific ozone dose of 20 mg ozone/mg nitrobenzene. The results are represented in Fig. 1.

As shown in Fig. 1, the concentrations of nitrobenzene all decrease with the increasing reaction time in the processes of ozonation alone, ozonation/ceramic honeycomb and ozonation/Mn–ceramic honeycomb. The degradation efficiency of nitrobenzene is higher in the presence of ceramic honeycomb catalyst compared to the case of ozonation alone, and the highest degradation efficiency of nitrobenzene is observed for combined ozone and Mn–ceramic honeycomb. In order to evaluate adsorption of nitrobenzene on the surface of catalyst, the experiments were conducted under the same experimental conditions as used in the previous tests but with the absence of ozone. It is also observed in Fig. 1 that the degradation of 2% and 3% is only detected in the processes of adsorption by ceramic honeycomb and Mn–ceramic honeycomb catalyst, respectively. Compared with the experimental results of ozonation alone and catalyzed ozonation processes, adsorption of nitrobenzene was too little to have important contribution to the degradation efficiency of nitrobenzene, and the modification of ceramic honeycomb by loading Mn can slightly enhance adsorption of nitrobenzene on the catalyst surface.

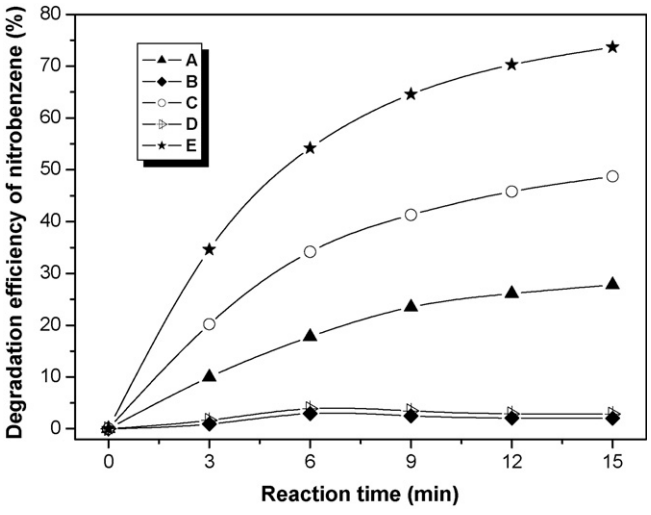

Fig. 1. Comparison of the degradation efficiency of nitrobenzene in the different processes (reaction conditions—temperature: 293 K; initial pH: 6.92; terminal pH 6.89–6.91; initial nitrobenzene concentration: 50 μg L^{-1}; the concentration of total applied ozone: 1.00 mg L^{-1}; the amount of ceramic honeycomb and 2.00% Mn–ceramic honeycomb catalysts used, respectively, in catalytic ozonation: 58.3 and 60.3 g L^{-1}; (A) ozonation alone; (B) adsorption of ceramic honeycomb; (C) ozonation/ceramic honeycomb; (D) adsorption of Mn–ceramic honeycomb; (E) ozonation/Mn–ceramic honeycomb).

In addition, comparing ozonation/ceramic honeycomb (the curve C) with the cumulative effect of ozonation alone and adsorption of ceramic honeycomb (the curves A and B), an increment of approximately 19% of nitrobenzene degradation is observed. Under the same experimental conditions, ozonation/Mn–ceramic honeycomb system leads to about 74% nitrobenzene conversion, indicating that an increment of 43% compared to the cumulative effect of ozonation alone and adsorption of Mn–ceramic honeycomb. The phenomenon indicates that the presence of ceramic honeycomb or Mn–ceramic honeycomb catalyst has the synergistic effect with ozone for the degradation of nitrobenzene, respectively, and the modification process can improve the catalytic activity of ceramic honeycomb for ozonation of nitrobenzene.

It is now widely assumed that ozone reacts in aqueous solution on various organic and inorganic compounds, either by direct, selective reactions of molecular ozone or through a radical type reaction involving •OH induced by ozone decomposition in water [38,39]. Since the oxidizing potential of •OH is much higher than that of molecular ozone, •OH is a less selective and more powerful oxidant than molecular ozone, and it is one of the most reactive free radicals and one of the strongest oxidants [40]. The reaction rate of •OH with organic molecules is usually in the order of 10^6 to 10^9 M^{-1} s^{-1} [41]. The reaction rate constant of nitrobenzene with •OH is 2.2×10^8 M^{-1} s^{-1} [42], while the rate constant for reaction of nitrobenzene with ozone alone is only 0.09 ± 0.02 M^{-1} s^{-1} [43]. Therefore, the results of Fig. 1 maybe suggest that nitrobenzene is degraded mainly by •OH oxidation in the processes of ozonation alone and catalytic ozonation.

3.2. Influence of *tert*-butanol on degradation efficiency of nitrobenzene

In order to identify preliminarily the reaction mechanism of the degradation of nitrobenzene in the processes of ozonation alone and catalytic ozonation, the experiments were carried out to compare the degradation efficiency of nitrobenzene obtained in the presence of *tert*-butanol with that in the case of its absence. The experimental results are shown in Fig. 2.

As indicated in Fig. 2, the presence of *tert*-butanol in aqueous solution has a remarkable influence on the degradation efficiency of nitrobenzene in the processes of ozonation alone and catalytic ozonation, leading to the significant reduction of degradation efficiency. With the increasing additional concentration of *tert*-butanol from 0 to 12 mg L^{-1}, the degradation efficiency of nitrobenzene decreases by 24%, 39% and 61% in the processes of ozonation alone, ozonation/ceramic honeycomb and ozonation/Mn–ceramic honeycomb, respectively.

Being a stronger radical scavenger, *tert*-butanol has the reaction rate constant of 5.0×10^8 M^{-1} s^{-1} with •OH [44] and 3.0×10^{-3} M^{-1} s^{-1} with ozone alone [43]. *tert*-Butanol reacts with •OH and generates inert intermediates, which do not predominantly produce the $HO_2^{\bullet}$ and $O_2^{\bullet -}$ radicals, thus causing the termination of the radical chain reaction. Comparing the reaction rate constant of •OH with *tert*-butanol to that with nitrobenzene, it can be found that the latter is lower than the former by 2.3 times.

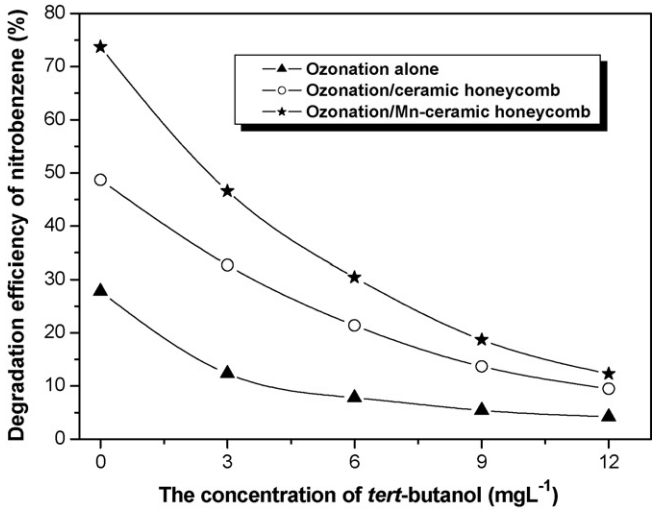

Fig. 2. Effect of ***tert***-butanol on the degradation efficiency of nitrobenzene in the different processes (reaction conditions—temperature: 293 K; initial pH 6.92; terminal pH: 6.89–6.91; initial nitrobenzene concentration: 50 μg L^{-1}; the concentration of total applied ozone: 1.00 mg L^{-1}; the amount of ceramic honeycomb and 2.00% Mn–ceramic honeycomb catalysts used, respectively, in catalytic ozonation: 58.3 and 60.3 g L^{-1}; the concentration of ***tert***-butanol: 0, 3, 6, 9 and 12 mg L^{-1}; reaction time: 15 min).

Therefore, due to the higher reaction rate constant and initial concentration (0–12 mg L^{-1}) selected by the experiment, *tert*-butanol is believed to be a relatively suitable indicator for radical type reaction produced in the present oxidative systems. The results of this experiment present that the addition of different concentration of *tert*-butanol all has a negative influence on the degradation efficiency of nitrobenzene in the three processes, indicating that *tert*-butanol traps competitively and consumes rapidly •OH in aqueous solution, which is the main drawback of all oxidative degradation processes based on •OH reactions. The results also suggest that nitrobenzene is oxidized primarily by •OH in the processes of ozonation alone, ozonation/ceramic honeycomb and ozonation/Mn–ceramic honeycomb.

The previous study found that, under the present experimental conditions of reaction temperature and initial pH, ozone alone reacts with nitrobenzene mostly through a radical type reaction involving •OH induced by the ozone self-decomposition in aqueous solution [26]. As far as catalytic ozonation is concerned, it may be assumed that the initiation of •OH is enhanced by the introduction of heterogeneous catalytic surface.

3.3. Influence of the variables on degradation efficiency of nitrobenzene

The variables can influence significantly the degradation efficiency of nitrobenzene in the ozonation experiments performed in the present study. Otherwise, they are very important to the practical operation of organic compounds removal in wastewater treatment and drinking water supply with source water of the river and the lake. Therefore, the experiments investigated preliminarily the influences of basal variables on the degradation efficiency of nitrobenzene.

3.3.1. Amount of catalyst

Heterogeneous catalytic ozonation of nitrobenzene in aqueous solution is a reaction system of gas–liquid–solid three phases, in which the solid catalyst is a crucial factor affecting the degradation efficiency. Firstly, it is necessary to assess the influence of amount of catalyst. The degradation efficiency of nitrobenzene was investigated by the catalytic ozonation in the presence of different amount of ceramic honeycomb and Mn–ceramic honeycomb catalysts. The results illustrate that the degradation efficiency of nitrobenzene increases gradually and positively by 23% and 51%, respectively, with the increasing amount of catalysts (0–81.7 g L^{-1}) in the processes of ozonation/ceramic honeycomb and ozonation/Mn–ceramic honeycomb. It is also possible that the increase of amount catalyst enhances the heterogeneous catalytic surface, leading to the increase of •OH initiation which improves the degradation efficiency of nitrobenzene. As illuminated by the results, the increase of the catalyst amount from 58.3 to 81.7 g L^{-1} yields a slow further increase of the degradation efficiencies of nitrobenzene in the both processes.

3.3.2. Reaction temperature

A series experiment of the degradation of nitrobenzene was carried out at different reaction temperature in the processes of ozonation alone and catalytic ozonation. The influence of reaction temperature on the degradation of nitrobenzene is shown in Fig. 3.

As indicated in Fig. 3, reaction temperature is an important factor on the degradation of nitrobenzene, whether in the ozonation alone system or in the catalytic ozonation systems. The degradation efficiency of nitrobenzene increases remarkably by 34%, 39% and 25% with the increasing reaction temperature (283–323 K) in the processes of ozonation alone, ozonation/ceramic honeycomb and ozonation/Mn–ceramic honeycomb, respectively. It can be concluded that the influence of reaction temperature is positive to the degradation efficiency in the range of 283–323 K. However, when reaction temperature is further increased up to 313 and 323 K, only a slight increase was observed in the three processes mentioned above, and the degradation efficiency almost reaches respectively a plateau in the both ozonation alone and ozonation/Mn–ceramic honeycomb systems. The anomalous phenomenon is due to the balance of two aspects corresponding to this experiment. On the one hand, ozone solubility in aqueous solution decreases with the increasing reaction temperature. On the other hand, an increase of reaction temperature should yield an increase in the reaction rate constant of the chemical reaction rate [45]. Both opposite effects lead to the similar synthetic results of the degradation efficiency of nitrobenzene in the processes of ozonation alone, ozonation/

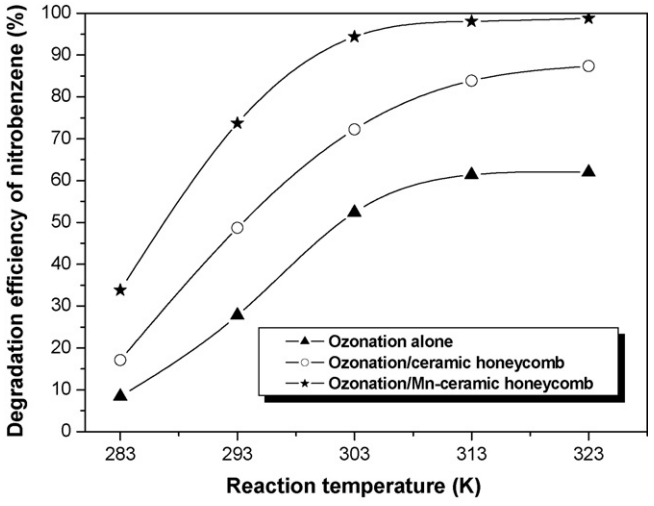

Fig. 3. Effect of reaction temperature on the degradation efficiency of nitrobenzene in the different processes (reaction conditions—temperature: 283, 293, 303, 313 and 323 K; initial pH 6.92; terminal pH: 6.89–6.91; initial nitrobenzene concentration: 50 μg L^{-1}; the concentration of total applied ozone: 1.00 mg L^{-1}; the amount of ceramic honeycomb and 2.00% Mn–ceramic honeycomb catalysts used, respectively, in catalytic ozonation: 58.3 and 60.3 g L^{-1}; reaction time: 15 min).

ceramic honeycomb and ozonation/Mn–ceramic honeycomb with the reaction temperature scope of 283–323 K, which are shown in Fig. 3.

3.3.3. Initial pH

The degradation efficiency of nitrobenzene in aqueous solution was investigated by conducting an experimental series at different initial pH in the processes of ozonation alone and catalytic ozonation. Fig. 4 depicts the influence of initial pH.

As observed, the degradation efficiency of nitrobenzene in aqueous solution is greatly increased with the increasing initial pH range from 2.89 to 12.46 in the ozonation alone system at reaction temperature 293 K. However, only in the initial pH range 2.89–8.83, the degradation efficiency of nitrobenzene in the ozonation/ceramic honeycomb system can follow this positive influence rule, and the increasing initial pH to 10.67 and 12.46 result in a reduction of the degradation efficiency compared to that of initial pH 8.83 in the same system. Otherwise, the degradation efficiency of nitrobenzene in the ozonation/Mn–ceramic honeycomb system is consistent with the result of ozonation alone in the initial pH range 2.89–10.67, which is a positive influence trend, and eventually obtains a slight decrease at initial pH 12.46. Therefore, from the results of Fig. 4 it is deduced that the optimum operation pH is located respectively in the proximity of 8.83 and 10.67 to the processes of ozonation/ceramic honeycomb and ozonation/Mn–ceramic honeycomb.

For the ozonation alone system, the influence of initial pH on the degradation efficiency of nitrobenzene comes from the action of pH on the homogeneous ozonation. Firstly, ozone is very unstable in aqueous solution due to its high active resonance structures of molecule. The half-life time of ozone molecular varies from a few seconds up to few minutes and depends on pH, water temperature and concentration of organic and inorganic compounds in aqueous solution [39]. Secondly, since in the ozone decomposition mechanism the active species is the conjugate base HO_2^- whose concentration is strictly dependent upon pH. The increase of pH will thus result into higher rates of $^{\bullet}OH$ production and the attainment of higher steady-state concentrations of $^{\bullet}OH$ in the radical chain decomposition process [46]. Furthermore, the major secondary oxidant formed from ozone decomposition in aqueous solution is the $^{\bullet}OH$ [47]. Therefore, the influence of initial pH is evident, which is a faster degradation efficiency contributed by $^{\bullet}OH$ oxidation at high pH levels as observed in Fig. 4.

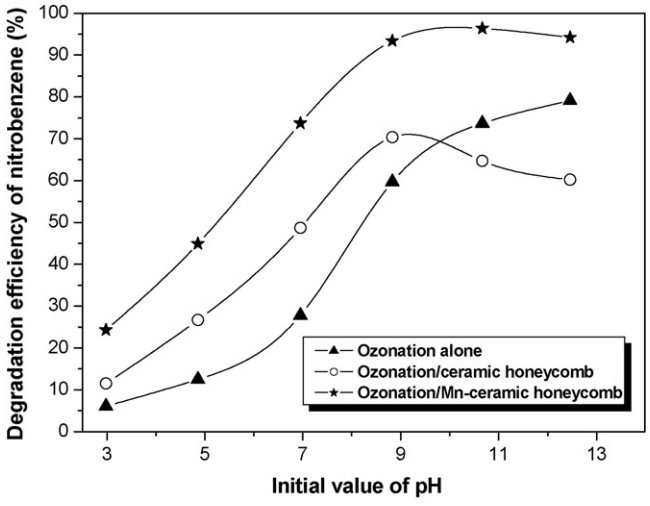

Fig. 4. Effect of initial value of pH on the degradation efficiency of nitrobenzene in the different processes (reaction conditions—temperature: 293 K; initial pH: 2.98, 4.86, 6.92, 8.83, 10.67 and 12.46; initial nitrobenzene concentration: 50 μg L^{-1}; the concentration of total applied ozone: 1.00 mg L^{-1}; the amount of ceramic honeycomb and 2.00% Mn–ceramic honeycomb catalysts used, respectively, in catalytic ozonation: 58.3 and 60.3 g L^{-1}; reaction time: 15 min).

Comparing the results of catalytic ozonation with those of ozonation alone mentioned above, it can be found that the degradation efficiencies of nitrobenzene in both the processes of catalytic ozonation are favoured from the synergistic effect of homogeneous and heterogeneous catalytic ozonation, the latter of which is based on the introduction of heterogeneous catalytic surface. Consequently, the discrepant trend of higher initial pH in catalytic ozonation systems should be ascribed to the deactivation of heterogeneous catalyst because of effective components leaching [48]. Further work will be planned to investigate deeply the influence mechanism of the variables mentioned above and the influences of other variables on the degradation efficiency of nitrobenzene. Simultaneously, the result also shows the obvious difference between the catalytic ozonation and the conventional ozonation alone, which is mainly attributed to the initiation effect of heterogeneous catalytic surface.

3.4. The surface characteristics of the catalysts

Because of the significant role of heterogeneous catalyst to the catalytic ozonation of gas–liquid–solid three phases, the surface characteristics of ceramic honeycomb and Mn–ceramic honeycomb catalysts were investigated in the experiment. The result of XRD analysis identifies that the bulk crystalline phase of ceramic honeycomb catalyst is $2MgO–2Al_2O_3–5SiO_2$, which is the standard structure of α-cordierite. Comparing to the result obtained with the raw ceramic honeycomb catalyst, the modification of ceramic honeycomb by loading Mn leads to the appearance of additional peaks of MnO_2. Furthermore, the specific surface area values are evaluated by BET method, revealing a remarkable increase of the specific surface area from 0.352 $m^2\ g^{-1}$ of ceramic honeycomb to 2.548 $m^2\ g^{-1}$ of 2.0% Mn–ceramic honeycomb, namely more than seven times higher than the surface area of the raw ceramic honeycomb catalyst. The introduction of Mn, as the modifier, also changes the pH_{PZC} from 6.60 of the raw catalyst to 6.82 of 2.0% Mn–ceramic honeycomb. In addition, due to the loading percentage of Mn was selected in the experiment within a relatively lower concentration range, resulting in an unapparent conversion of pH_{PZC}. The examination results show that the surface hydroxyl groups of 0.91×10^{-5} and 2.56×10^{-5} mol m^{-2} exist, respectively, on the surface of ceramic honeycomb and 2.0% Mn–ceramic honeycomb catalyst.

It is reported that heterogeneous catalytic ozonation is a potential alternative AOP because the presence of heterogeneous surface appears to transfer ozone into aqueous solution more efficiently [49]. Therefore, the changes of the surface characteristics of catalyst must result in the evolution of ozone transformation.

3.5. The utilization efficiency of ozone in the different processes

Considering the significant influence of ozone transformation step on the ozonation reaction, the experiment examined the evolution of ozone mass transfer in the processes of ozonation alone and catalytic ozonation. Ozone mass transformation is composed of several parts, including the concentration of total applied ozone ($[O_3]_T$), the concentration of residual ozone ($[O_3]_R$), the concentration of offgas ozone ($[O_3]_O$) and the concentration of consumed ozone ($[O_3]_C$). As a matter of convenience to evaluate, the dimension of all parts mentioned above is transferred uniformly from milligram to milligram per liter. Therefore, mass balance of ozone between gas and liquid phase can be formulated as follows:

$$[O_3]_T = [O_3]_O + [O_3]_R + [O_3]_C \quad (1)$$

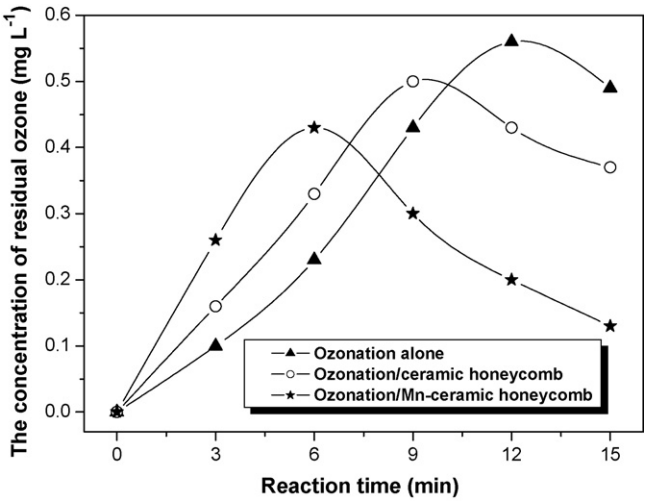

Fig. 5. Evolution of the concentration of residual ozone in the different processes (reaction conditions—temperature: 293 K; initial pH: 6.92; terminal pH: 6.89–6.91; initial nitrobenzene concentration: 50 μg L^{-1}; the concentration of total applied ozone: 1.00 mg L^{-1}; the amount of ceramic honeycomb and 2.00% Mn–ceramic honeycomb catalysts used, respectively, in catalytic ozonation: 58.3 and 60.3 g L^{-1}).

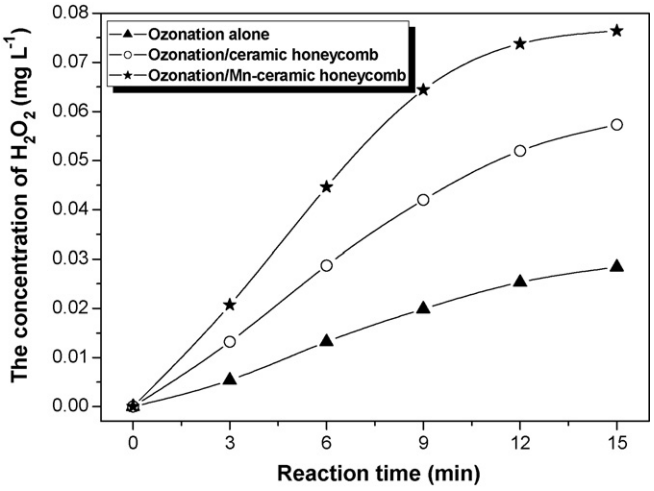

Fig. 6. Comparison of the concentration of H_2O_2 formation in the different processes (reaction conditions—temperature: 293 K; initial pH: 6.92; terminal pH: 6.89–6.91; initial nitrobenzene concentration: 50 μg L^{-1}; the concentration of total applied ozone: 1.00 mg L^{-1}; the amount of ceramic honeycomb and 2.00% Mn–ceramic honeycomb catalysts used, respectively, in catalytic ozonation: 58.3 and 60.3 g L^{-1}).

Firstly, the variation of $[O_3]_R$ was practically identified in the different processes within reaction time of 15 min. The results are presented in Fig. 5.

The results of Fig. 5 depict that $[O_3]_R$ reaches the maximum of 0.56 mg L^{-1} in the process of ozonation alone at 12 min, and then decreases to 0.49 mg L^{-1} at 15 min reaction time. While $[O_3]_R$ in the ozonation/ceramic honeycomb and ozonation/Mn–ceramic honeycomb systems present the maximum value of 0.50 and 0.30 mg L^{-1} at about 9 min and 6 min, respectively. After that time point, $[O_3]_R$ in the both processes decline steadily to 0.37 and 0.13 mg L^{-1} with the increase of reaction time to 15 min.

Secondly, $[O_3]_O$ was measured under the same experimental conditions. The results indicate that $[O_3]_O$ of ozonation alone is the highest among those of the three processes, and that of ozonation/Mn–ceramic honeycomb is the lowest. Based on the data of Fig. 5 and $[O_3]_O$, $[O_3]_C$ can be calculated from Eq. (1). Therefore, R_U, the utilization efficiency of ozone can be expressed as follows:

$$R_U = \frac{[O_3]_C}{[O_3]_T} \quad (2)$$

According to the results obtained and Eq. (2), the evolution of R_U corresponding to the experimental processes studied can be obtained. It is found that the evolution of R_U follows the contrary rule of $[O_3]_O$ in the processes of ozonation alone, ozonation/ceramic honeycomb and ozonation/Mn–ceramic honeycomb. It is also demonstrated that ceramic honeycomb has the catalytic activity to enhance R_U, and the modification of ceramic honeycomb with Mn further improves this activity. The phenomena of the experiments, which are the decrease of $[O_3]_R$ and the increase of R_U in the three processes, suggest that the presence of heterogeneous surfaces may be also help to initiate the production of novel oxidative intermediate species from ozone decomposition [49].

3.6. The production of oxidative intermediate species from ozone decomposition

There are some intermediate species production occur as known from chemistry of ozonation in aqueous solution. Due to the high complexity of chemical reactions, highly oxidative species are often classified as the so-called oxidative intermediate species. Many research work monitor hydrogen peroxide produced in some AOPs involving ozone [50–52]. To investigate H_2O_2 formation generated from ozone decomposition, the accumulation of H_2O_2 concentration in aqueous solution were observed in the three processes. The results are shown in Fig. 6.

As given in Fig. 6, certain concentrations of H_2O_2 are formed as a result of ozone decomposition, and the concentration of H_2O_2 formation increases continuously to 0.0284, 0.0573 and 0.0764 mg L^{-1} with increasing reaction time to 15 min in the processes of ozonation alone, ozonation/ceramic honeycomb and ozonation/Mn–ceramic honeycomb, respectively. Fig. 6 also demonstrates that, with addition of ceramic honeycomb catalyst, the formation of H_2O_2 is more obvious compared to the case of ozonation alone. Furthermore, the formation of H_2O_2 becomes more pronounced in the presence of Mn–ceramic honeycomb catalyst.

In addition, due to the reaction corresponding to H_2O_2 in the presence of ozone, as listed below [46,53,54], there should be $^{\bullet}OH$ formation initiated in the selected processes.

$$3O_3 + 2H_2O_2 \rightarrow 2^{\bullet}OH + 3O_2 \quad (3)$$

$$H_2O_2 + O_3 \rightarrow {}^{\bullet}OH + HO_2^{\bullet} + O_2 \quad (4)$$

Some previous studies find that $^{\bullet}OH$ is formed in the process of heterogeneous catalyst ozonation [29,45,55]. The experiment determined the formation of $^{\bullet}OH$ by means of spin-trapping/electron paramagnetic resonance (EPR) technique, which can detect unstable radicals by measuring the intensity of DMPO-OH adduct signal, in the processes of ozonation alone, ozonation/ceramic honeycomb and ozonation/Mn–ceramic honeycomb. The results are summarized in Fig. 7.

From Fig. 7, it is seen that the typical EPR spectrum appears, respectively, in the selected processes at the initial DMPO concentration of 100 mmol. The spectrum is composed of quartet lines having a peak height ratio of 1:2:2:1 and the parameters are hyperfine constants α_N = 1.49 mT, α_H = 1.49 mT and g-value = 2.0055. These parameters coincide with those of the DMPO-OH adduct as demonstrated previously [56]. The phenomenon of the experiment indicates that $^{\bullet}OH$ initiation exists in the

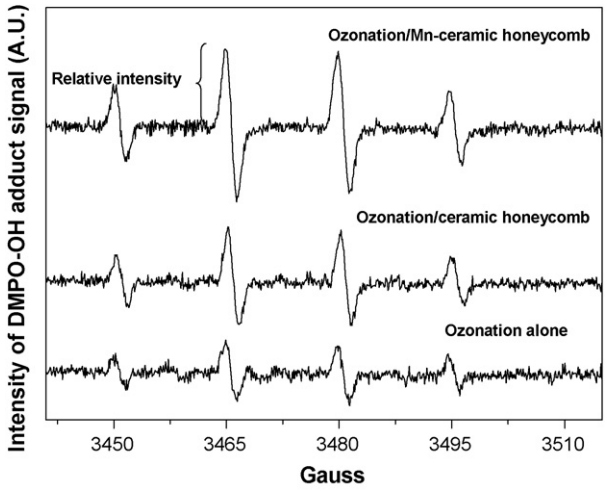

Fig. 7. Comparison of the intensity of DMPO-OH adduct signal in the different processes (reaction conditions—temperature: 293 K; initial pH: 6.92; terminal pH: 6.89–6.91; initial nitrobenzene concentration: 50 μg L^{-1}; the concentration of total applied ozone: 1.00 mg L^{-1}; the amount of ceramic honeycomb and 2.00% Mn–ceramic honeycomb catalysts used, respectively, in catalytic ozonation: 58.3 and 60.3 g L^{-1}; initial DMPO concentration: 9.6 g L^{-1}).

three processes mentioned above. In fact, •OH can be scavenged by itself to produce H_2O_2 through the •OH termination reaction [21,57,58].

$$^{\bullet}OH + {}^{\bullet}OH \rightarrow H_2O_2 \quad (5)$$

It also can be found that the DMPO-OH adduct signal observed in the catalytic ozonation systems are stronger than the case of ozonation alone. Like H_2O_2 formation, the results of Fig. 7 also suggest that the processes of ozonation/ceramic honeycomb and ozonation/Mn–ceramic honeycomb can generate higher concentration of •OH under the same experimental conditions compared to that obtained from the ozonation alone system due to the introduction of heterogeneous surface, which can affect significantly the degradation mechanism of ozonation.

3.7. Discussion on reaction mechanism of catalytic ozonation process

The chemistry of ozone in aqueous solution is complex. Ozone molecular can oxidize water impurities via direct, selective reactions or can undergo decomposition via a chain reaction mechanism resulting in the generation of •OH [39]. Based on the previous research [26] and the results mentioned above, it is deduced that ozonation alone for the degradation of nitrobenzene is mainly attributed to the •OH oxidation, which is initiated from the self-decomposition of ozone in aqueous solution under this experimental conditions. The results also suggest that the introduction of ceramic honeycomb increases the ozonation degradation of nitrobenzene by improving the initiation of •OH and the modification with Mn further increases the catalytic activity of the raw ceramic honeycomb catalyst. Catalytic ozonation in the experiment is difficult to be completely understood owing to the synergistic effect of homogeneous and heterogeneous catalytic ozonation. The experiment focused more attention on the enhancement mechanism of heterogeneous catalytic ozonation by Mn–ceramic honeycomb.

At first, the increase of catalytic activity is ascribed to the impregnation of Mn, suggesting that Mn is the effective component of catalytic activity improvement. The results of the influence of loading percentage of Mn on the degradation efficiency of nitrobenzene present that, as shown in Fig. 8(a), the higher loading percentages of Mn result in the higher degradation

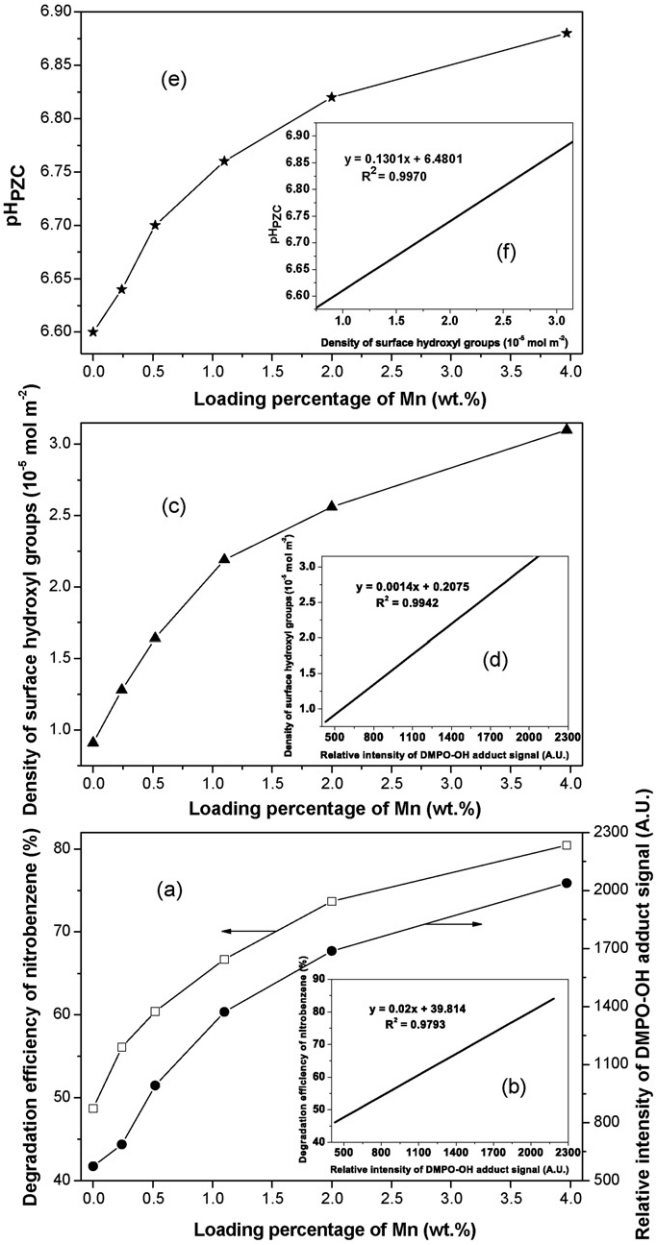

Fig. 8. The conversion of degradation efficiency of nitrobenzene, relative intensity of DMPO-OH adduct signal, density of surface hydroxyl groups and pH_{PZC} with the loading percentage of Mn (reaction conditions—temperature: 293 K; initial pH: 6.92; terminal pH: 6.89–6.91; initial nitrobenzene concentration: 50 μg L^{-1}; the concentration of total applied ozone: 1.00 mg L^{-1}; the amount of Mn–ceramic honeycomb catalysts used in catalytic ozonation: 58.3 g L^{-1}; loading percentage of Mn (wt.%): 0, 0.25, 0.50, 1.00, 2.00 and 4.00%; initial DMPO concentration: 9.6 g L^{-1}; (a) the conversion of degradation efficiency of nitrobenzene and relative intensity of DMPO-OH adduct signal with the loading percentage of Mn; (b) the relationship between degradation efficiency of nitrobenzene and relative intensity of DMPO-OH adduct signal at the different loading percentage of Mn; (c) the conversion of density of surface hydroxyl groups with the loading percentage of Mn; (d) the relationship between density of surface hydroxyl groups and relative intensity of DMPO–OH adduct signal at the different loading percentage of Mn; (e) the conversion of pH_{PZC} with the loading percentage of Mn; (f) the relationship between pH_{PZC} and density of surface hydroxyl groups at the different loading percentage of Mn).

efficiencies. Simultaneously, relative intensity of DMPO-OH adduct signals also increase with the increasing of loading percentages of Mn, meaning that higher concentrations of •OH are initiated in the case of higher loading percentages of Mn. Furthermore, a relative good correlation is apparent from Fig. 8(b) showing the relationship between the degradation efficiency of nitrobenzene between

relative intensity of DMPO-OH adduct signal. This phenomenon demonstrates that the higher degradation efficiency of nitrobenzene is due to the higher concentration of $^{\bullet}OH$ oxidation, which derives from the higher loading percentage of Mn in the process of ozonation/Mn–ceramic honeycomb. The experimental results also further confirm that the reactions follow the mechanism of $^{\bullet}OH$ oxidation, as described in Figs. 2 and 7. And it is interesting to note that the surface hydroxyl group on heterogeneous catalytic surface plays an important role to initial $^{\bullet}OH$ from ozone decomposition [29].

When the catalyst made up of metal oxides, such as $2MgO–2Al_2O_3–5SiO_2$ and MnO_2, are introduced into aqueous solution, H_2O molecules will be strongly adsorbed on the metal oxides surface. The adsorbed H_2O always dissociate into OH^- and H^+, forming surface hydroxyl groups with surface cations and oxygen anions, respectively [59]. Then, the chemisorbed surface hydroxyl groups characterize the oxide/water interface. It is generally believed that dissolved ozone adsorbs first on the catalyst's surface and then decomposes rapidly due to presence of surface hydroxyl group. Because of the decomposition of ozone, active atomic oxygen is produced and reacts with surface hydroxyl group to HO_2^- anions which subsequently can react very fast with another O_3 to O_2H radicals or the O_2H radicals can be produced directly. This radical reacts subsequently with another ozone molecule to generate an O_3^- radical. The O_3^- radical decomposes into oxygen and a $^{\bullet}OH$ which can oxidize organic compounds either in solution or on the surface or in a thin film layer above the catalyst's surface [60]. Another research work finds that ozone can react with the surface hydroxyl group, initiating the production of $^{\bullet}OH$ on the surface of the catalyst [29].

Furthermore, as the oxidative intermediate species from ozone decomposition, H_2O_2 and $^{\bullet}OH$ determined in reaction systems (Figs. 6 and 7) can indicate the series complex matrix reactions, which occur mainly in the homogeneous aqueous phase after the initiation step from the heterogeneous catalytic surface. Firstly, those species formed in the initiation and propagation steps can scavenge $^{\bullet}OH$ through the termination reaction step, which listed as follows [21,47,53,57,58,60–68]:

$$^{\bullet}OH + O_3 \rightarrow HO_2^{\bullet} + O_2 \quad (6)$$

$$^{\bullet}OH + O_3 \rightarrow HO_4^{\bullet} \quad (7)$$

$$^{\bullet}OH + HO^- \leftrightarrow H_2O + O^{\bullet -} \quad (8)$$

$$^{\bullet}OH + HO_2^- \rightarrow HO_2^{\bullet} + HO^- \quad (9)$$

$$^{\bullet}OH + HO_2^- \rightarrow O_2^- + H_2O \quad (10)$$

$$^{\bullet}OH + HO_2^{\bullet} \rightarrow H_2O + O_2 \quad (11)$$

$$^{\bullet}OH + O_2^{\bullet -} \rightarrow HO^- + O_2 \quad (12)$$

Simultaneously, H_2O_2 can be formed through the $^{\bullet}OH$ termination reactions (13–15) except for reaction (5) [21,58,64].

$$^{\bullet}OH + {}^{\bullet}OH \rightarrow H_2O_2 + O_2 \quad (13)$$

$$^{\bullet}OH + HO_3^{\bullet} \rightarrow H_2O_2 + O_2 \quad (14)$$

$$^{\bullet}OH + HO_4^{\bullet} \rightarrow H_2O_2 + O_3 \quad (15)$$

The buildup of H_2O_2 is also reduced by its own termination reactions (16–20) shown below, some of which can produce $^{\bullet}OH$ through reactions (16–18) [53,54,57,63,64].

$$H_2O_2 + O_3 \rightarrow {}^{\bullet}OH + HO_2^{\bullet} + O_2 \quad (16)$$

$$H_2O_2 + HO_2^{\bullet} \rightarrow {}^{\bullet}OH + H_2O + O_2 \quad (17)$$

$$H_2O_2 + O_2^{\bullet -} \rightarrow {}^{\bullet}OH + HO^- + O_2 \quad (18)$$

$$H_2O_2 + O_3 \rightarrow H_2O + O_2 \quad (19)$$

$$H_2O_2 \leftrightarrow HO_2^- + H^+ \quad (20)$$

In addition, it is interesting to emphasize that $^{\bullet}OH$ can react with H_2O_2 to finish their termination step and the initiation of $HO_2^{\bullet}$ [21,54,57,62,64,66,68].

$$^{\bullet}OH + H_2O_2 \rightarrow HO_2^{\bullet} + H_2O \quad (21)$$

Therefore, the results of Figs. 6 and 7 represent the equilibriums concentrations of $^{\bullet}OH$ and H_2O_2 in the selected processes. Based on the measurement of density of surface hydroxyl groups on Mn–ceramic honeycomb catalyst, the conversion of density of surface hydroxyl groups was investigated with the loading percentage of Mn in the experiment. The results are schematized in Fig. 8(c).

The results shown in Fig. 8(c) represent that, the higher the loading percentage of Mn, the higher is the density of surface hydroxyl groups, indicating that the density of surface hydroxyl groups is dependent on the loading percentage of Mn which is the modifier. Otherwise, Fig. 8(d) depicts the relationship of density of surface hydroxyl groups and relative intensity of DMPO-OH adduct signal at the different loading percentage of Mn, showing a good correlation. The linearity listed in Fig. 8(d) means that $^{\bullet}OH$ is generated from the series complex matrix reactions of surface hydroxyl group with ozone including the initiation, the propagation and the termination steps. It is also to be noted that density of surface hydroxyl groups can be significantly influenced by pH_{PZC}.

pH_{PZC} is the zero charge point of the pH, at which the amounts of negative and positive surface charges developed by proton equilibrium are equivalent. Firstly, pH_{PZC} was detected at different loading percentage of Mn in the experiment. The results are summarized in Fig. 8(e).

Fig. 8(e) depicts the conversion of pH_{PZC} with the loading percentage of Mn, indicating that the increase of loading percentage of Mn results in the increase of pH_{PZC}. At the same time, Fig. 8(f) presents the relationship of pH_{PZC} and density of surface hydroxyl groups at the different loading percentage of Mn, also showing a very good positive correlation. In addition, the surface hydroxyl groups have different charge states depending on the pH of aqueous solution. When the pH is near pH_{PZC} of the oxide, most of the surface hydroxyl groups will be at neutral state. Otherwise, protonated or deprotonated surface hydroxyl groups predominate when the pH of aqueous solution is far below or above the pH_{PZC}. However, only the surface hydroxyl groups at neutral state are believed to have a relative higher catalytic activity to accelerate the initiation of $^{\bullet}OH$ and the decomposition of ozone [27]. Under the present experimental condition of initial pH 6.92, the increase of loading percentage of Mn can lead to the increase of density of surface hydroxyl groups at neutral state due to the closer pH_{PZC} to pH of aqueous solution (see Fig. 8(f)), because the conversion of pH produced by the degradation of 50 $\mu g\,L^{-1}$ nitrobenzene may scarcely affect the level of pH and can therefore be neglected. Therefore, the enhancement mechanism of heterogeneous catalytic ozonation by Mn–ceramic honeycomb is obvious.

Firstly, the loading of Mn can lead to the increase of pH_{PZC} and the enhancement of density of surface hydroxyl groups, which can cause the improvement of density of surface hydroxyl groups at neutral state due to the closer pH_{PZC} to pH of aqueous solution. Secondly, the improvement of density of surface hydroxyl groups, special at neutral state can accelerate the decomposition of ozone and the initiation of $^{\bullet}OH$, resulting in the increase of degradation efficiency of nitrobenzene.

Further research work is still needed to investigate the initiation efficiency of •OH by the surface hydroxyl groups at different charge states and the adjustment of surface characteristics by the modification of catalyst.

4. Conclusions

It has been demonstrated that the degradation efficiency of nitrobenzene in aqueous solution by ozonation alone is accelerated in the presence of ceramic honeycomb and Mn–ceramic honeycomb as the catalysts, and the more pronounced degradation efficiency is achieved in the process of ozonation/Mn–ceramic honeycomb. The results suggest that the adsorption of the organic model substances on the surface of catalysts is not compulsory for effective catalytic ozonation, in fact it may scarcely be attributed to the increased level of nitrobenzene degradation and can therefore be neglected compared to that of catalytic ozonation.

The experiments with addition of *tert*-butanol (0–12 mg L^{-1}), a well-known •OH scavenger, confirm that nitrobenzene is oxidized primarily by •OH in the processes of ozonation alone, ozonation/ceramic honeycomb and ozonation/Mn–ceramic honeycomb. The degradation efficiency of nitrobenzene is always enhanced by increasing amount of ceramic honeycomb and Mn–ceramic honeycomb catalyst (0–81.7 g L^{-1}), respectively. The increasing of reaction temperature (283–323 K) can enhance the degradation efficiency of nitrobenzene in the three processes. The degradation efficiency of nitrobenzene increases as initial pH is increased (2.89–12.46) in the process of ozonation alone, and reaches, respectively, the maximum at initial pH 8.83 and 10.67 in the processes of ozonation/ceramic honeycomb and ozonation/Mn–ceramic honeycomb. The modification of ceramic honeycomb with Mn leads to the formation of new crystalline phase of MnO_2, and increases the specific surface area, pH_{PZC} and density of surface hydroxyl groups. The utilization efficiency of ozone, the formation of H_2O_2 and the initiation of •OH are all significantly improved in the catalytic ozonation compared to the non-catalytic ozonation, and the improvements of them in the presence of Mn–ceramic honeycomb are even more pronounced than those of raw ceramic honeycomb.

The investigation of reaction mechanism indicates that the loading of Mn can cause the increase of pH_{PZC} and the enhancement of density of surface hydroxyl groups, resulting in the acceleration of ozone decomposition and the initiation of •OH, leading to the increase of degradation efficiency of nitrobenzene.

Acknowledgement

The authors gratefully acknowledge the financial support from National Natural Science Foundation of China (Grant No. 50578051).

References

[1] R. Mantha, K.E. Taylor, N. Biswas, J.K. Bewter, Environ. Sci. Technol. 35 (2001) 3231–3236.
[2] Y. Mu, H.Q. Yu, J.C. Zheng, S.J. Zhang, G.-P. Sheng, Chemosphere 54 (2004) 789–794.
[3] J.S. Zhao, O.P. Ward, P. Lubicki, J.D. Cross, P. Huck, Biotechnol. Bioeng. 73 (2001) 306–312.
[4] S. Contreras, M. Rodríguez, E. Chamarro, S. Esplugas, J. Photochem. Photobiol. A: Chem. 142 (2001) 79–83.
[5] J. Sarasa, M.P. Roche, M.P. Ormad, E. Gimeno, A. Puig, J.L. Ovelleiro, Water Res. 32 (1998) 2721–2727.
[6] L.S. Bell, J.F. Devlin, R.W. Gillham, P.J. Binning, J. Contam. Hydrol. 66 (2003) 201–217.
[7] M. Rodriguez, V. Timokhin, F. Michl, S. Contreras, J. Gimenez, S. Esplugas, Catal. Today 76 (2002) 291–300.
[8] D. Bahnemann, in: O. Hutzinger, P. Boule (Eds.), The Handbook of Environmental Chemistry, Springer, Berlin, 1999, pp. 285–351.
[9] D.S. Bhatkhande, V.G. Pangarkar, A.A. Beenackers, J. Chem. Technol. Biotechnol. 77 (2001) 102–116.
[10] R. Dillert, M. Brandt, I. Fornefett, U. Siebers, D. Bahnemann, Chemsphere 30 (1995) 2333–2341.
[11] M. Rodríguez, A. Kirchner, S. Contreras, E. Chamarro, S. Esplugas, J. Photochem. Photobiol. A: Chem. 133 (2000) 123–127.
[12] S.J. Zhang, S.H. Feng, H.Q. Yu, Q.R. Li, J. Environ. Sci. 16 (2004) 364–366.
[13] T. Gorontzy, J. Kuver, K.H. Blotevogel, J. Gen. Microbiol. 139 (1993) 1331–1336.
[14] D. Mansuy, P. Beaune, T. Crestell, C. Bacot, J.C. Chottard, P. Gans, Eur. J. Biochem. 86 (1978) 573–579.
[15] A. Schackmann, R. Muller, Appl. Microbiol. Biotechnol. 34 (1991) 809–813.
[16] C.Z. Thompson, L.E. Hill, J.K. Epp, G.S. Probst, Environ. Mutagen. 5 (1983) 803–811.
[17] R.J. Tayade, R.G. Kulkarni, R.V. Jasra, Ind. Eng. Chem. Res. 45 (2006) 922–927.
[18] D.S. Bhatkhande, V.G. Pangarkar, A.A.C.M. Beenackers, Water Res. 37 (2003) 1223–1230.
[19] M. Rodriguez, A. Kirchner, S. Contreras, E. Chamarro, S. Esplugas, J. Photochem. Photobiol. A 133 (2000) 123–127.
[20] I. Arslan-Alaton, J.L. Ferry, Appl. Catal. B: Environ. 38 (2002) 283–293.
[21] F.J. Beltrán, J. Rivas, P.M. Álvarez, M.A. Alonso, B. Acedo, Ind. Eng. Chem. Res. 38 (1999) 4189.
[22] Y.X. Yang, J. Ma, Q.D. Qin, X.D. Zhai, J. Mol. Catal. A: Chem. 267 (2007) 41–48.
[23] J. Ma, M.H. Sui, Z.L. Chen, L.N. Wang, Ozone Sci. Eng. 26 (2004) 3–10.
[24] J. Ma, M.H. Sui, T. Zhang, C.Y. Guan, Water Res. 39 (2005) 779–786.
[25] Z.Z. Sun, J. Ma, L.B. Wang, L. Zhao, J. Environ. Sci. 17 (2005) 716–721.
[26] L. Zhao, J. Ma, Z.Z. Sun, Appl. Catal. B: Environ. 79 (2008) 244–253.
[27] T. Zhang, J. Ma, J. Mol. Catal. A: Chem. 279 (2007) 82–89.
[28] J. Ma, N.J.D. Graham, Ozone Sci. Eng. 19 (1997) 227–233.
[29] J. Ma, N.J.D. Graham, Water Res. 33 (1999) 785–793.
[30] J. Ma, N.J.D. Graham, Water Res. 34 (2000) 3822–3828.
[31] K.L. Rakness, G. Gordon, B. Langlais, W. Masschelein, N. Matsumoto, Y. Richard, C.M. Robson, I. Somiya, Ozone Sci. Eng. 18 (1996) 209–229.
[32] H. Bader, J. Hoigné, Water Res. 15 (1981) 449–456.
[33] H. Bader, V. Sturzenegger, J. Hoigné, Water Res. 22 (1988) 1109–1115.
[34] E. Laiti, L.O. Öhman, J. Nordin, S. Sjöberg, J. Colloid Interface Sci. 175 (1995) 230–238.
[35] H. Tamura, A. Tanaka, K.Y. Mita, R. Furuichi, J. Colloid Interface Sci. 209 (1999) 225–231.
[36] J.S. Noh, J.A. Schwarz, J. Colloid Interface Sci. 130 (1989) 157–164.
[37] J.S. Noh, J.A. Schwarz, Carbon 28 (1990) 675–682.
[38] B. Legube, V.L.N. Karpel, Catal. Today 53 (1999) 61–72.
[39] B. Kasprzyk-Hordern, M. Ziółek, J. Nawrocki, Appl. Catal. B: Environ. 46 (2003) 639–669.
[40] C.P. Huang, C. Dong, Z. Tang, Waste Manage. 13 (1993) 361–377.
[41] R. Andreozzi, V. Caprio, A. Insola, R. Marotta, Catal. Today 53 (1999) 51–59.
[42] J. Hoigné, H. Bader, Water Res. 10 (1976) 377–386.
[43] J. Hoigné, H. Bader, Water Res. 17 (1983) 173–183.
[44] G. Bablon, W.D. Bellamy, M.M. Bourbigot, in: B. Langlais, D.A. Reckhow, D.R. Brink (Eds.), Ozone in Water Treatment: Application and Engineering, Lewis Publishers, Chelsea, Michigan, USA, 1991, pp. 11–132.
[45] F.J. Beltrán, F.J. Rivas, R. Montero-de-Espinosa, Appl. Catal. B: Environ. 39 (2002) 221–231.
[46] W.H. Glaze, J.W. Kang, Ind. Eng. Chem. Res. 28 (1989) 1573–1580.
[47] U. von Gunten, Water Res. 37 (2003) 1443–1467.
[48] M. Carbajo, F.J. Beltrán, F. Medina, O. Gimeno, F.J. Rivas, Appl. Catal. B: Environ. 67 (2006) 177–186.
[49] C. Cooper, R. Burch, Water Res. 33 (1999) 3695–3700.
[50] E. Mvula, C. von Sonntag, Org. Biomol. Chem. 1 (2003) 1749–1756.
[51] J.W. Kang, M.R. Hoffmann, Environ. Sci. Technol. 32 (1998) 3194–3199.
[52] J.W. Kang, H.-M. Hung, A. Lin, M.R. Hoffmann, Environ. Sci. Technol. 33 (1999) 3199–3205.
[53] K. Sehested, H. Corfitzen, J. Holcman, E.J. Hart, J. Phys. Chem. A 102 (1998) 2667–2672.
[54] E. Neyens, J. Baeyens, J. Hazard. Mater. B 98 (2003) 33–50.
[55] B.S. Kim, H. Fujita, Y. Sakai, A. Sakoda, M. Suzuki, Water Sci. Technol. 46 (2002) 35–41.
[56] H. Utsumi, M. Hakoda, S. Shimbara, H. Nagaoka, Y. Chung, A. Hamada, Water Sci. Technol. 30 (1994) 91–99.
[57] U. von Gunten, Y. Oliveras, Environ. Sci. Technol. 32 (1998) 63–70.
[58] J. Staehelin, R.E. Buhler, J. Hoigné, J. Phys. Chem. 88 (1984) 5999–6004.
[59] Y. Joseph, W. Ranke, W. Weiss, J. Phys. Chem. B 104 (2000) 3224–3236.
[60] M. Ernst, F. Lurot, J.C. Schrotter, Appl. Catal. B Environ. 47 (2004) 15–25.
[61] J. Staehelin, J. Hoigné, Environ. Sci. Technol. 16 (1982) 676–681.
[62] F.J. Beltrán, M. González, B. Acedo, F.J. Rivas, J. Hazard. Mater. B 80 (2000) 189–206.
[63] T.E. Agustina, H.M. Ang, V.K. Vareek, J. Photochem. Photobiol. C: Photochem. Rev. 6 (2005) 264–273.
[64] M. Pera-Titus, V. García-Molina, M.A. Baños, J. Giménez, S. Esplugas, Appl. Catal. B Environ. 47 (2004) 219–256.
[65] J. Staehelin, J. Hoigné, Environ. Sci. Technol. 19 (1985) 1206–1213.
[66] F. Xiong, J.P. Croué, B. Legube, Environ. Sci. Technol. 26 (1992) 1059–1064.
[67] Y.G. Adewuyi, Environ. Sci. Technol. 39 (2005) 8557–8570.
[68] H.S. Christensen, H. Sehestd, H. Corfitzan, J. Phys. Chem. 86 (1982) 15–88.